PROBA-2 Attitude and Orbit Control System: In-Flight Results of Innovative GNC Functions

J. Côté*, A. Kron*, J. de Lafontaine*, J. Naudet**, S. Santandrea***

*NGC Aerospace Ltd, 1650, rue King Ouest, Office 202, Sherbrooke, Québec, Canada
** Qinetiq Space nv, Belgium
*** ESA/ESTEC, Noordwijk, the Netherlands

Abstract: The PRoject for On-Board Autonomy (PROBA) is an ESA technology-demonstration program aimed at the in-orbit validation of autonomy-enabling space technologies. Following the success of PROBA-1, the PROBA-2 spacecraft was launched on 2 November 2009 and continues the in-flight demonstration of on-board autonomy by performing a Sun observation mission as well as numerous flight experiments. This paper completes previously published articles by presenting the in-flight results of two innovative autonomous GNC functions: (1) Star Tracker Earth Exclusion Angle Prediction for Earth avoidance and (2) Large-Angle Rotation around Fixed Axis. Finally, flight results of the Attitude and Orbit Control System (AOCS) nominal operation using these innovative GNC functions will be presented.

Keywords: Attitude and Orbit Control System, Guidance, Navigation and Control System, attitude estimation and control, attitude perturbation, Extended Kalman Filter, sliding-mode controller.

1. INTRODUCTION

The PRoject for On-Board Autonomy (PROBA) is a European Space Agency (ESA) technology-demonstration program aimed at the in-orbit validation of autonomy-enabling space technologies. Following the success of PROBA-1 (de Lafontaine et al., 1999, Teston et al., 2007), the PROBA-2 spacecraft was launched on 2 November 2009 from Plezetsk as secondary passenger on board a Rockot launcher. It was delivered to the client, ESA, in February 2010 after a successful commissioning campaign. Since then, PROBA-2 performs its nominal Sun observation mission.

The on-board Attitude and Orbit Control System (AOCS) software developed by NGC Aerospace Ltd (NGC) is at the heart of the intelligence of the spacecraft providing it with the unique capability to autonomously enable functions and operational modes without ground support.

This paper is the continuation of five previously published papers regarding the development and validation of the PROBA-2 Attitude and Orbit Control System (AOCS) software. The design of the autonomous Guidance, Navigation and Control (GNC) algorithms required for the basic mission operations as well as the GNC technology experiments to be validated in flight was presented in a paper for the 6th International ESA Conference on GNC systems (de Lafontaine et al., 2005). Simulation results of the critical GNC functions were presented in an ASTRO 2006 paper (de Lafontaine et al., 2006). A subsequent ASTRO 2008 paper reported the lessons learned during the integration of the AOCS software and the system-level tests (de Lafontaine et al., 2008a). At the 7th International ESA Conference on GNC systems in June 2008, a fourth paper was published describing the validation activities that were conducted to qualify the AOCS software for flight and presenting the results of these activities for critical functions of the AOCS software (de Lafontaine et al., 2008b). A fifth paper was published reporting the flight validation results obtained during the AOCS commissioning (Côté et al., 2010a). Finally a sixth paper has been presented at the 8th International ESA Conference on GNC systems describing the validation in flight of the AOCS flight experiments implemented on-board by NGC Aerospace (Côté et al., 2011).

Now that the AOCS software has been fully documented and commissioned, this paper presents flight results obtained during the nominal operation of the AOCS software. This paper first provides an overview of the PROBA-2 mission. The AOCS software functional scheme and the different operational modes are reviewed. The flight results of two innovative GNC functions critical for the PROBA-2 nominal operation are then presented. Finally, in-flight results of the PROBA-2 nominal operation are described with emphasis on the contributions of the two innovative GNC functions mentioned above.

2. OVERVIEW OF THE PROBA-2 MISSION

The PROBA-2 spacecraft, mission, AOCS software structure, modes and pointing requirements have been widely presented in papers cited in introduction. This section only provides a summary of the mission and AOCS modes in order to support the reader with the upcoming sections.

2.1 PROBA-2 Mission Overview

For PROBA-2, the second generation of autonomous software has been adapted to a Sun observation mission. The spacecraft evolves on a 725-km Sun-synchronous, dawn-dusk

orbit with ascending node at 6 AM. This orbit maximises the duration of the season without eclipse (about 286 days per year) for best Sun observation. This mission is controlled from Redu ground station in Belgium.

The spacecraft has the capability to autonomously perform periodic large-angle rotations in order to avoid blinding of the star sensor by the Earth. This feature allows undisrupted measurements to execute accurate pointing to specific regions of the Sun.

In addition to the software-based experiments, PROBA-2 is used to the demonstration in a real mission scenario of a wide range of space technologies including payloads for future operational missions:

- SWAP: Sun Watcher using APS detectors and image Processing to observe the Sun ultra-violet light.
- LYRA: Lyman Alpha Radiometer to analyse ultra-violet bands using novel diamond detectors.
- DSLP: Dual Segmented Langmuir Probe to measure electron temperature.
- TPMU: Thermal Plasma Measurement unit also to measure electron temperature.

Fig. 1: Artist View of PROBA-2 Fully Operational

2.2 PROBA-2 AOCS Software Overview

The PROBA-2 AOCS software can be activated in 6 operational modes. Transition between any of them is possible and can be commanded either by the ground station or, autonomously, by the on-board mission manager. The Bdot and Sun modes are the most critical enabling the System Safe mode and Sun observation mode required to provide an autonomous Sun-observation scientific mission. These modes are briefly described now.

In **Bdot mode,** the interaction with the magnetic field is used to reduce spacecraft angular rates. This is the main rate reduction mode to remove the excess angular rate imparted to the spacecraft at separation. It also serves as the fallback safe mode in cases of anomalies.

In **Inertial mode**, the attitude is controlled with respect to the inertial frame. It is used mainly for calibration.

In **Orbital mode**, the attitude is controlled with respect to the orbital frame for geocentric pointing.

In **Flight mode**, the attitude is controlled with respect to the orbital velocity to allow propulsion manoeuvres.

In **Earth-target mode**, the attitude is controlled to point a target on Earth.

In **Sun mode**, the attitude is controlled with respect to the Sun frame. N ($2 \leq N \leq 8$) times an orbit, the satellite performs autonomous periodic, fast large-angle rotation about the payload line of sight, in order to avoid star tracker blinding. As shown in the next figure, those large-angle rotations are performed around the Sun direction vector. This mode is the main observation mode of the mission. It requires specific innovations discussed in the next section.
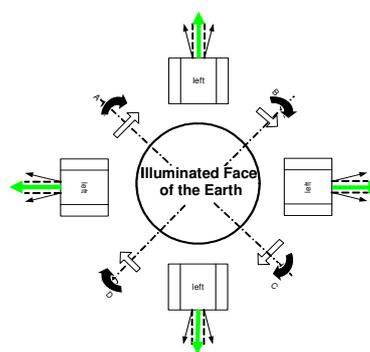

Fig. 2: Autonomous Large-Angle Rotations around the Sun Vector (Star Tracker in Dark Green)

3. INNOVATIVE GNC FUNCTIONS FLIGHT RESULTS

With the dawn-dusk, near-polar orbit and the need to continuously point payloads to the Sun, the only practical configuration for the star sensors is to align them at 90 deg to the Sun direction. Hence, periodic blinding of the sensors by the Earth is unavoidable unless the spacecraft is rotated around the Sun line as shown above.

On the one hand, some payloads requires a fixed attitude with respect to the Sun and accept a limited number of N minimum-time large-angle rotations around the Sun line to avoid star sensor blinding by the Earth. On the other hand, other payloads require a continuous and accurate pointing to the Sun even during the fast large-angle manoeuvres. Therefore, the AOCS software must not only perform a fast, minimum-time, large-angle rotation between two specific attitudes, it must also do so while pointing the rotation axis accurately to the Sun.

This requires predicting and tracking the attitude that maximises the Earth Exclusion Angle (EEA) of the star sensor while keeping an accurate pointing toward a specific region of the Sun. This is ensured by the means of two innovative functions discussed in this section.

3.1 Star Tracker Earth Exclusion Angle Prediction for Earth Avoidance

As introduced above and shown in Fig. 2, N minimum-time large-angle rotations around the Sun line need to be commanded every orbit of the Sun Observation mode. To do so, the EEA is used to monitor and predict if and when the star sensors will be blinded by the Earth. The EEA is defined

as the angle between the sensor line of sight and the Earth atmosphere (de Lafontaine et al., 2005, 2006).

These predictions are performed on board by the EEA prediction function described in de Lafontaine et al. (2005). Simulation results were provided in Lafontaine et al. (2006). This section gives equivalent flight results.

Eight candidate attitudes are provided to the AOCS software along with an index (i.e. from 1 to 8). The AOCS software predicts the EEA for each of these candidates as well as the current and next best candidates which maximises the EEA. It returns the corresponding index to the System along with the predicted remaining time until the best candidate attitude will change. Based on these predictions, the System commands the most appropriate candidate attitude at the right time in order to avoid the STR to be blinded by the Earth. The EEA prediction function also estimates the current EEA for safety monitoring.

Fig. 3 shows the flight results obtained on 01 April 2011 for the predicted and estimated EEA. Four candidate attitudes were provided and predicted accordingly. The predicted EEA are shown with blue lines whereas the estimate of the current EEA is shown in green. The figure shows that the candidate attitudes successively provide the best EEA while the current EEA follows the best candidate. The large-angle manoeuvre required to reach the next best candidate attitude can be observed in Fig. 3 whenever the current EEA estimates (the green line) leaves a blue a line (the current best candidate attitude) to track another blue line (the next best candidate attitude).

As explained above, a large-angle rotation is commanded by the System a few seconds before the current best candidate attitude provides a worse EEA than the next best (See Fig. 3). The on-board prediction of the current and next best candidate attitude is shown on the top graph of Fig. 4. The time until the next best candidate is required by the System to autonomously command the large-angle rotation required to reach a new candidate attitude. This predicted time too is shown on the bottom graph of Fig. 4.

These flight results demonstrate the performance and the functionality of the EEA prediction used for the nominal operation of the PROBA-2 spacecraft.
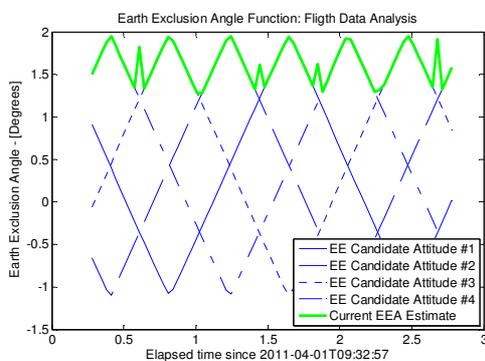

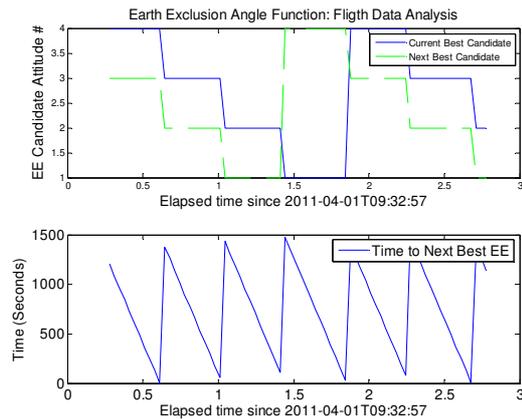Fig. 3: Earth Exclusion Angle Prediction and Estimation

Fig. 4: Predicted Current and Next Best Candidate Attitude: Index (top) and Time to next best (bottom)

3.2 Large-Angle Rotation around Fixed Axis

As explained in introduction of Section 3 the AOCS software must not only perform a fast, minimum-time, large–angle rotation between two specific attitudes in order to track the selected EEA, it must also do so while pointing the rotation axis accurately to the Sun. Indeed, the co-alignment between the payload boresight vector and the Sun target vector (i.e. pointing direction to a specific region of the Sun) during the large-angle rotations shall be smaller than 1 deg.

This problem of fixed axis rotation has been solved by enhancing the PROBA-1 sliding-mode controller (details in de Lafontaine et al., 2008a). While, the PROBA-1 controller tracked only a reference angular-velocity defines as a function of the reference sliding surface in the phase plan, here an additional feedback is implemented in order to co-align the angular rate vector with the reference fixed-axis. This control is enhanced by gyroscopic torque cancellation.

Fig. 5 built with flight data presents the angle between the payload boresight vector and Sun direction vector.
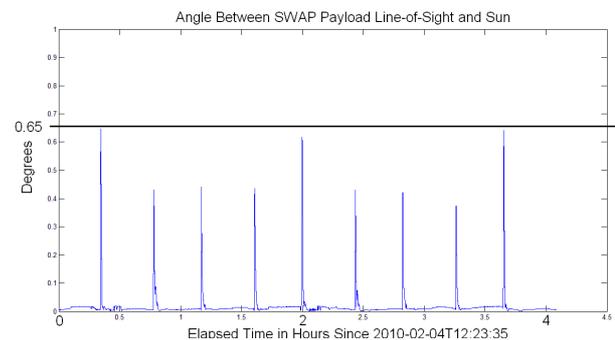

Fig. 5: Pointing Error during Large-Angle Rotations (Requirements: < 1 degree)

Each peak occurs during a large–angle rotation. The horizontal line characterizes the maximum deflection (0.65 deg.). Thus, this figure highlights that the co-alignment deflection always remains in the specification range (1 deg.) including during the large-angle rotation such that the

payload can keep on measuring without loss of scientific data. In turn, this validates the enhanced sliding-mode controller that perform rotation around a commanded fixed axis

4. AOCS NOMINAL OPERATION FLIGHT RESULTS

In order to fulfil its mission, the spacecraft operates in Sun Observation mode pointing toward the Sun and performing the periodic rotations by taking advantage of the two innovative algorithms presented above. In this context, beyond the 1 deg. co-alignment specification, the AOCS software has to fulfill the following pointing and measurement performance specifications. Note that "arcsec" refers to arc-seconds.

Nominal pointing performance specifications in Sun observation mode:

- Absolute Measurement Accuracy (AMA): 10 arcsec (2σ)

- Absolute Pointing Error (APE): 100 arcsec (2σ)

- Relative Pointing Error (RPE): 5 arcsec over 5 s (2σ)

Goal pointing performance specifications in Sun mode (nice to have):

- Relative Pointing Error (RPE): 1 arcsec over 60 sec (1σ)

This sections reports and analyses flight data that related to these requirements. First, estimation results are presented. Then, pointing performance is discussed.

4.1 States Estimation

At the heart of the PROBA-2 AOCS navigation function, two Extended Kalman Filter (EKF) are implemented in order to provide the autonomy required by the PROBA missions: a GPS-based EKF for orbital state estimation and a star sensor (STR)-based EKF for attitude estimation.

The PROBA-2 EKFs are based on the PROBA-1 EKFs into which lessons learned from the analysis of PROBA-1 flight performance were implemented to enhance its performance, functionality and the robustness. The estimation filters developed for PROBA-1 was fully described in de Lafontaine et al., 1999.

The orbital and attitude EKF are implemented into two different functions in order to avoid the dependence on each other. The orbital EKF provides the spacecraft position and velocity with respect to the Earth Centered Inertial (ECI) frame. The attitude EKF provides the spacecraft body rate attitude quaternion with respect to the ECI. The attitude also provides the wheels angular momentum estimated from the wheel speed measurement. However, the attitude filter can work normally without those measurements or in presence of wheel failures.

The orbital filter is based on time-tagged GPS measurements whereas the attitude filter is based on time-tagged STR measurements. The time tags provided with each set of

measurements are used by a closed-loop delay-recovery algorithm in order to actualise the measurement to the time of estimation.

The flight performance of both filters is now analysed. Evidently, such estimation performance cannot be evaluated in flight since a better source of knowledge does not exist. On ground, it is evaluated with high-fidelity simulator of the spacecraft. In flight, the filter's residues provide the best indication of the filter performance and stability with respect to the measurement. The filter residues actually correspond to the error between the *a priori* filter estimate and the measurement.

The following graph gives the flight results for the orbital state estimates (inertial position) and residues.
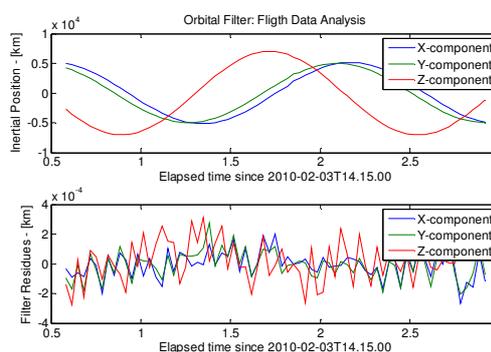

Fig. 6: Inertial Position Estimation and Filter's residues

In Markgraf et al., 2010, it was demonstrated that the GPS yield accuracy of from 0.06 to 1.2 m per axis (i.e. overall 3D rms position accuracy of 2 m). From this graph, it can be concluded that the on-board orbital filter properly averages out these measurements as the residues correspond to the measurement noise.

The following graphs give the flight results for the attitude state estimates and residues.
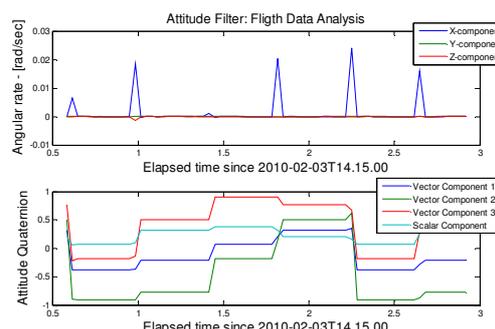

Fig. 7: Spacecraft Angular Rate and Attitude Quaternion Estimates

The attitude state estimates clearly show the effect of the large-angle rotations commanded autonomously to maximise the EEA. The peaks seen in the top graph of Fig. 7 correspond to the spacecraft rate during the large-angle rotation. The estimation attitude quaternion corresponds to

the selected best candidate attitude predicted by the EEA function addressed in Section 3.1.

The figure below shows the attitude filter residues respectively around the STR line-of-sight and the around the axis perpendicular to it.
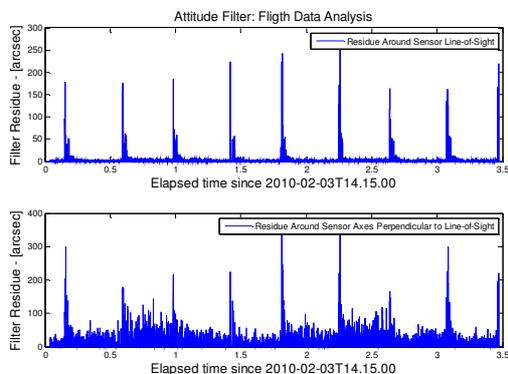

Fig. 8: Spacecraft Attitude Filter Residues

During the commissioning of the star sensor, it was identified that the star sensor noise, in the flight configuration, was about 3 and 24 arcsec respectively around the STR line-of-sight and around the axis perpendicular to it. From the graph above, it can be concluded that the on-board attitude filter properly averages out the STR measurement as the residues correspond to the measurement noise. The regular peak corresponds to the large-angle rotation during which the attitude filter is converging to the new attitude. This behavior is normal since some star sensor measurements are invalid during fast manoeuvre and as the attitude filter is tuned to be highly averaging in order to meet the mission requirements.

These flight results obtained from the GPS-based orbit estimation function and from the STR-based attitude estimation function demonstrate the performance of the EKF used by the PROBA-2 AOCS navigation function for orbit and attitude estimation.

4.2 Attitude Pointing Performance

The pointing performance before any in-flight tuning and calibration is illustrated in Fig. 9. The top graph shows the APE where the performance specification is indicated by a green horizontal line. A maximum APE of about 100 arcsec was observed, with peaks exceeding 200 arcsec. The bottom graph shows the RPE also with the performance specification indicated. It can be observed that the RPE exhibits peaks that are correlated with APE peaks. The large peaks going out of the figure at regular interval (e.g. 0.5h, 0.9h, 1.3h, 1.7h etc.) are generated by the large-angle rotation of 90 degrees that are performed four times per orbit to avoid star tracker blinding. These peaks must not be considered during assessment of the performance.

The cause for the peaks in Fig. 9 was traced to the misalignment between the two star tracker heads. When attitude control autonomously switches from using one head, the other or both, the misalignment causes a change in the

attitude. The AOCS software however has the capability to autonomously estimate this misalignment and compensate for it. After enabling this functionality, the pointing performance looked much better (Fig. 10).

All the peaks beyond the limit of performance are removed, and the RPE also is well within the requirements. Nevertheless, during some parts of the orbit, there remain peaks of 30 arcsec for the RPE. This is caused by the reaction wheel momentum offloading. The offloading is performed by switching on the magnetic torquers, and the resulting disturbances are not compensated for. Consequently, the offloading function has been tuned in order to reduce the offloading occurrences at a level compatible with the mission (Côté et al., 2010).

The pointing performance was further improved by compensating for the satellite's Residual Magnetic Moment (RMM) disturbance which is the dominant attitude perturbation. This RMM was first estimated on ground. The AOCS software also implements a perturbation estimation function which autonomously estimates on board the RMM in order to improve the knowledge of the disturbances. Note that the RMM accounts for the largest contribution to these disturbances, more than that caused by solar pressure, drag and gravity gradient together. When the AOCS software compensates for the RMM, an average APE of 35 arcsec with maximum peak at 60 arcsec and an RPE of about 3 arcsec over 5s is obtained (Fig. 11).

The nominal requirements for the pointing performance of PROBA-2 are 100 arcsec absolute error and 5 arcsec (2σ) over 5s relative error. These requirements are easily met as shown in Fig. 11. The goal requirements (nice to have) specified a challenging RPE of 1 arcsec (1σ) over 60 seconds. This requirement is not fully met, although the RPE over a period of 60s is lower than 3arcsec for 78% of the time (against the specified 99.8%). This pointing performance is reported in Fig. 12 along with the indication where the large-angle rotations and/or momentum offloading occurred (red lines at the bottom).

These results shows that after careful tuning during the commissioning the mission requirements are met.
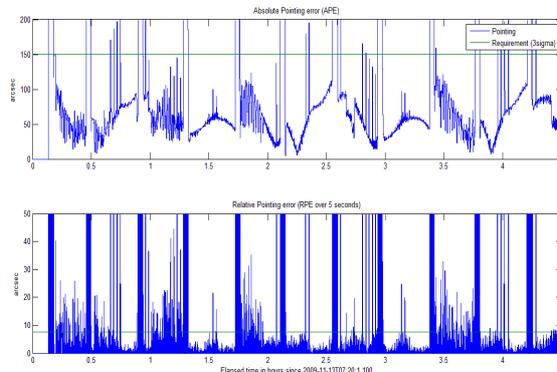

Fig. 9: Pointing Performance before On-Board Estimation of the Star Tracker Co-Alignment
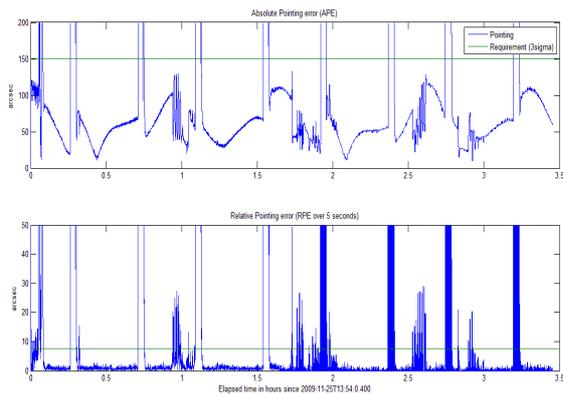
Fig. 10: Pointing Performance with Star Tracker Co-Alignment but without RMM Compensation
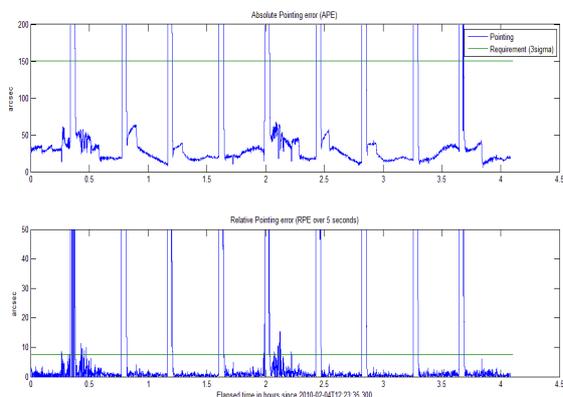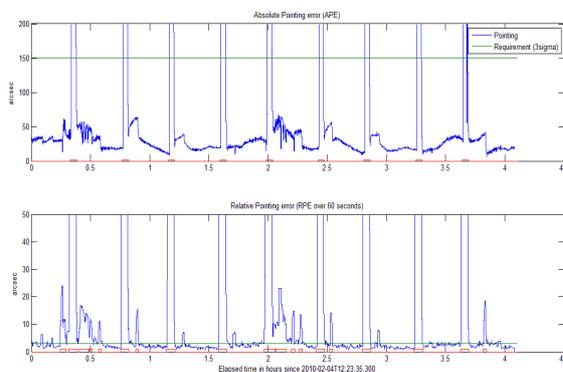

Fig. 11: Pointing Performance (Nominal)

Fig. 12: Pointing Performance (Target)

5. CONCLUSIONS

This paper focused on flight data analysis that demonstrates the in-flight performance of the autonomous AOCS software developed by NGC Aerospace Ltd. This on-board software implements innovative navigation, guidance and control algorithms that allow precision pointing toward the Sun while performing large-angle manoeuvre. Flight results demonstrate that after careful tuning during the commissioning, the performance requirements are met allowing the satellite performing its nominal mission. Beyond

this scientific mission, PROBA-2 tested also experimental GNC algorithms that have been presented in Côté et al., 2011.

6. AKNOWLEDGMENT

REFERENCE

Côté J., Kron A., Naudet J., de Lafontaine, J., Santandrea S., (2011). "PROBA-2 Attitude and Orbit Control System: In-Flight Results of AOCS Flight Experiments" *Proceedings of the 8th International ESA Conference on Guidance, Navigation and Control Systems*, Carlsbad, Czech Republic, Jun 5-10, 2011.

Côté J., Naudet J., Kron A., Santandrea S., de Lafontaine, J. (2010). "PROBA-2 Attitude and Orbit Control System: In-Flight Validation Results" *ASTRO 2010 - 15th Canadian Astronautics Conference*, Toronto, Ontario, Canada, May 4-6, 201*0*

de Lafontaine, J., Buijs J., Vuilleumier P. and Van den Braembussche P. (1999). "Development of the PROBA Attitude Control and Navigation Software", *Proc. 4th ESA International Conference on Spacecraft Guidance, Navigation and Control Systems, Noordwij*k, The Netherlands, 19-21 Oct. 1999.

de Lafontaine, J., Côté, J., Kron, A., Vuilleumier, P., Santandrea, S., and Van Den Braembussche, P. (2005). "Validation of Innovative State Estimation and Control Techniques on PROBA-2." *Proceedings of the 6th International ESA Conference on Guidance, Navigation and Control Systems*, Loutraki, Greece.

de Lafontaine, J., Côté, J., Kron, A., Vuilleumier, P., Santandrea, S., and Van Den Braembussche, P. (2006). "Innovative Autonomous Navigation and Control Functions On-Board the Mini-Satellite PROBA-2.", *ASTRO 2006 - 13th Canadian Astronautics Conference*, Montreal, Quebec, Canada, Apr. 25-28, 2006.

de Lafontaine, J., Côté, J., Kron, (2008a) "PROBA-2 Attitude and Orbit Control System: Lessons Learned from Integration and System-Level Tests", *ASTRO 2008 - 14th Canadian Astronautics Conference*, Montreal, Quebec, Canada, Apr. 26-May 01st, 2008.

de Lafontaine J., Côté J., Naudet J., Kron A., Santandrea S., (2008b) "PROBA-2: AOCS Software Validation Process and Critical Results," *Proceedings of the 7th International ESA Conference on Guidance, Navigation & Control Systems, Tralee*, County Kerry, Ireland, June 2-5, 2008

Markgraf M., Montenbruck, O., Santendrea, S. Naudet, J., "Phoenix-Gps Navigation System Onboard The Proba-2 Spacecraft –First Flight Results", Small Satellites Systems and Services- The 4S Symposium, 31 May – 4 June 2010, Madeira, Portugal (2010)

Teston, F., Vuilleumier, P., Hardy, D., Tilmans, E., Gantois, K., (2007). "PROBA Proves the Technology.", *ESA bulletin #129*